Amino Acids (2012) 42:1715–1725
DOI 10.1007/s00726-011-0882-6

ORIGINAL ARTICLE

Oostatic peptides containing D-amino acids: synthesis, oostatic activity, degradation, accumulation in ovaries and NMR study

Jan Hlaváček · Richard Tykva · Josef Holík · Blanka Bennettová · Miloš Buděšínský · Věra Vlasáková · Bohuslav Černý · Jiřina Slaninová

Received: 21 December 2010 / Accepted: 4 March 2011 / Published online: 18 March 2011

Abstract Analogs of the H-Tyr-Asp-Pro-Ala-Pro-OH pentapeptide with D-amino acid residues either in differing or in all of the positions of the sequences were prepared and their oostatic potency was compared with that of the parent pentapeptide. The D-amino acid residue containing analogs exhibited an equal or even higher oostatic effect in the flesh fly *Neobellieria bullata* than the parent peptide. Contrary to the rapid incorporation of radioactivity from the labeled H-Tyr-Asp-[^{3}H]Pro-Ala-Pro-OH pentapeptide into the ovaries of *N. bullata* in vitro, the radioactivity incorporation from the labeled pentapeptides with either D-aspartic acid or D-alanine was significantly delayed. As compared to the parent pentapeptide, also the degradation of both the D-amino acid-containing analogs mentioned above proceeded at a significantly lower rate. The decreased intake of radioactivity, the lower degradation and finally also the high oostatic effect may be ascribed to the decreased enzymatic degradation of the peptide bonds neighboring the D-amino acid residues in the corresponding peptides. The introduction of the non-coded D-amino acids thus enhances the oostatic effect in *N. bullata* owing to the prolonged half-life of the corresponding pentapeptides, which can thus affect more ovarian cells.

Keywords D-amino acids · Oostatic peptide synthesis · ^{3}H labeling · Oostatic activity in *Neobellieria bullata* · ^{3}H incorporation · Peptide degradation · NMR study

Abbreviations

AA	Amino acid analysis
AcOH	Acetic acid
ACN	Acetonitrile
APT	Attached proton test
COSY	Correlation spectroscopy
DIC	*N,N*-diisopropylcarbodiimide
DCM	Dichloromethane
DIEA	*N,N*-diisopropylethylamine
DMF	*N,N*-dimethylformamide
DMSO-d6	Dimethylsulfoxide-d6
ESI MS	Electro-spray ionization mass spectrometry
FAB MS	Fast atom bombardment mass spectrometry
Fmoc	[(Fluoren-1-yl-methoxy]carbonyl
HEPES	4-(2-hydroxyethyl)-1-piperazine-ethanesulfonic acid
HMBC	Heteronuclear multiple bond correlation
HOBt	1-Hydroxybenzotriazole
HSQC	Heteronuclear single quantum correlation
NOE	Nuclear Overhauser effect
ROESY	Rotating nuclear Overhauser effect spectroscopy
tBu	tert-butyl
TFA	Trifluoroacetic acid
TIS	Tri-isopropylsilane
TOCSY	Total correlation spectroscopy

The nomenclature and symbols of the amino acids follow the Recommendations of the IUPAC/IUB Joint Commission on Biochemical Nomenclature. Eur J Biochem 138:9–37 (1984).

J. Hlaváček (✉) · R. Tykva · M. Buděšínský · J. Slaninová
Institute of Organic Chemistry and Biochemistry, Academy of Sciences of the Czech Republic, Flemingovo nám. 2, 166 10 Prague 6, Czech Republic
e-mail: honzah@uochb.cas.cz

J. Holík · V. Vlasáková · B. Černý
Institute of Experimental Botany, Academy of Sciences of the Czech Republic, 142 20 Prague 4, Czech Republic

B. Bennettová
Institute of Entomology, Academy of Sciences of the Czech Republic, 370 05 České Budějovice, Czech Republic

Introduction

In our long-term study, we have been dealing with oostatic peptides structurally derived from the H-Tyr-Asp-Pro-Ala-Pro_6-OH decapeptide, which was isolated from a mosquito *Aedes aegypti* and described by Borovsky et al. 1990. This decapeptide was named TMOF—trypsin modulating oostatic factor—for its ability to regulate and terminate trypsin biosynthesis in the last phase of insect development.

We have found that TMOF also exhibits a mild oostatic effect in the flesh fly *Neobellieria bullata* and that its shortened analogs (Hlaváček et al. 1997, 1998, 2004) have this effect strongly enhanced (decreasing the hatchability of eggs and changing their structure, Fig. 1).

We subsequently used the ^{3}H-labeled form (**3a**) (see Table 1) of the most active pentapeptide **1a** in studies on its degradation and radioactivity accumulation in organs (ovaries, hemolymph) of the *N. bullata* (Tykva et al. 1999; Slaninová et al. 2004, 2007; Hlaváček et al. 2007). We found that the radioactivity incorporates into the organs in minutes and the pentapeptide is quickly degraded to tyrosine and the H-Asp-Pro-Ala-Pro-OH tetrapeptide in the ovaries and to proline and the H-Tyr-Asp-Pro-Ala-OH tetrapeptide in the hemolymph. The tetrapeptides further split into corresponding dipeptides with a final cleavage to a proline molecule.

In this study, we have focused our search on the oostatic effects of pentapeptides **1b–1g** (Table 1), containing D-amino-acid residues in either one or all of the positions of the parent oostatic pentapeptide structure (**1a**). Furthermore, we performed degradation and radioactivity accumulation studies on the selected pentapeptides **1c** and **1e** in the ovaries of the *N. bullata*, using their tritiated derivatives **3b** and **3c**, which we prepared from the corresponding precursors **2b** and **2c**, having dehydroproline ($^{\Delta}$Pro) in position 3. The results were further correlated with the data obtained from the NMR measurements in DMSO-d6.

Materials and methods

General methodologies

The protected amino acids were purchased from Bachem (Bubendorf, Switzerland) and the 2-chlorotrityl chloride resin (1.3 mmol/g) from Calbiochem-Novabiochem AG (Läufelfingen, Switzerland). The pentapeptide sequences with D-amino acids were assembled on the 2-chlorotrityl chloride resin using the AVPS-2 automatic peptide synthesizer (IOCB, ASCR, v.v.i., Prague, Czech Republic). The non-labeled truncated fragments of the pentapeptide sequence as the standards for the HPLC study have been prepared and described in our previous paper (Tykva et al. 2007). The samples for amino acid analysis were hydrolyzed with 6 M HCl containing 3% of phenol at 110°C for 20 h. The amino acid analyses were performed on a Biochrom 20 instrument (Pharmacia, Sweden). The molecular weights of the peptides were determined using a FAB MS (Micromass, Manchester, UK). For the HPLC of the non-labeled pentapeptides, a Spectra Physics instrument with an SP 8800 pump, an SP 4290 integrator and a Thermo Separation Products Spectra 100 UV detector were used. The

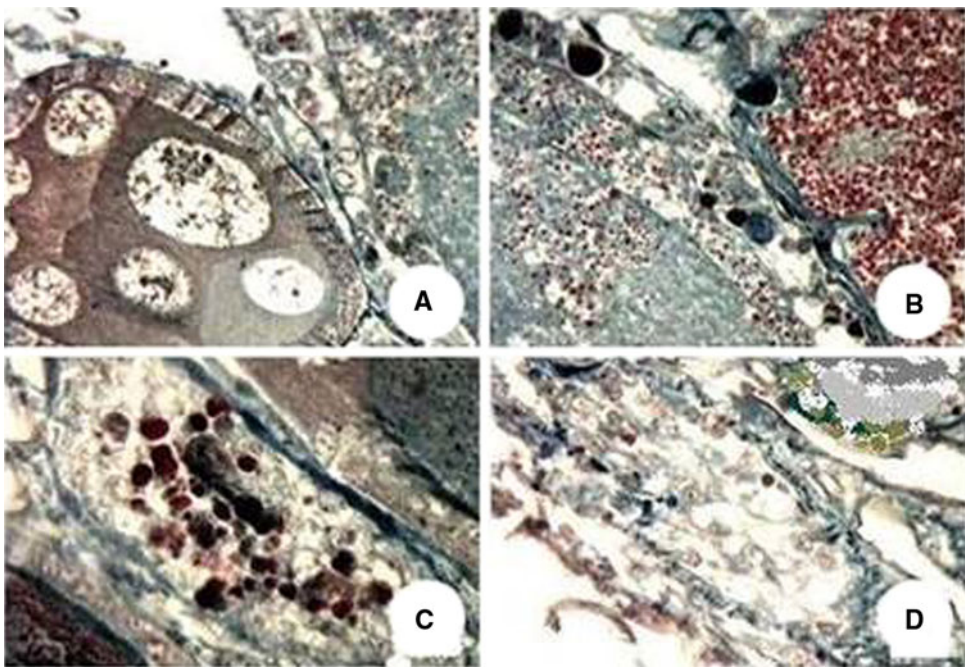

Fig. 1 The **o**ostatic effect of the H-Tyr-Asp-Pro-Ala-Pro-OH pentapeptide (**5P, 1a** in Table 1) on the flesh fly *Neobelliera bullata.* The monolayered follicular epithelium (**a**) divides, forming a multilayered structure (**b**) and filling the entire egg chamber (**c**), which degenerates and is resorbed (**d**)

Table 1 Structures of oostatic pentapeptide analogs

Pept. no.	Structure	Pept. no.	Structure
1a	H-Tyr-Asp-Pro-Ala-Pro-OH (5P)	**2a**	H-Tyr-Asp-$^{\Delta}$Pro-Ala-Pro-OH
1b	H-**D-Tyr**-Asp-Pro-Ala-Pro-OH	**2b**	H-Tyr-**D-Asp**-$^{\Delta}$Pro-Ala-Pro-OH
1c	H-Tyr-**D-Asp**-Pro-Ala-Pro-OH	**2c**	H-Tyr-Asp-$^{\Delta}$Pro-**D-Ala**-Pro-OH
1d	H-Tyr-Asp-**D-Pro**-Ala-Pro-OH	**3a**	H-Tyr-Asp-[^{3}H]Pro-Ala-Pro-OH
1e	H-Tyr-Asp-Pro-**D-Ala**-Pro-OH	**3b**	H-Tyr-**D-Asp**-[^{3}H]Pro-Ala-Pro-OH
1f	H-Tyr-Asp-Pro-Ala-**D-Pro**-OH	**3c**	H-Tyr-Asp-[^{3}H]Pro-**D-Ala**-Pro-OH
1g	H-**D-Tyr-D-Asp-D-Pro-D-Ala-D-Pro**-OH		

compounds were purified by a preparative HPLC on a 25 × 2.2 cm column, 10 μm Vydac RP-18 (The Separations Group, Hesperia, CA, USA), with a flow rate of 7 ml/min, detection at 220 nm using a 0–100% gradient of ACN in 0.05% aqueous TFA, for 120 min, unless otherwise stated. The analytical HPLC was carried out on a 15 × 0.4 cm column, 5 μm Supelco (Supelco, Bellefonte, PA, USA) with a flow rate of 1 ml/min, detection at 220 nm, using a 5–100 % gradient of ACN in 0.05 aqueous TFA, for 40 min. The NMR spectra were recorded on a Bruker AVANCE-600 spectrometer (Bruker BioSpin GmbH, Rheinstetten, Germany).

Preparation of the pentapeptides **1b–1g** and **2b**, **2c**

The Fmoc-Pro-OH and Fmoc-D-Pro-OH were loaded on the 2-chlorotrityl chloride resin (4 and 2 g, respectively) with a substitution of 0.43 mmol/g (Hlaváček et al. 1998), using the described procedure (Barlos et al.1991). The loaded resins were divided into six portions and, following a Fmoc deprotection by a 20% piperidine/DMF mixture (10 ml) for 20 and 30 min, each of the portions was separately acylated according to the given pentapeptide sequence with a fourfold excess (1.72 mmol) of a Fmoc-derivative of Ala or D-Ala (0.54 g), of Pro, D-Pro (0.58 g) or 3,4-$^{\Delta}$Pro (0.57 g), of Asp(OtBu) or D-Asp(OtBu) (0.71 g) and of Tyr(tBu) or D-Tyr(tBu) (0.79 g) using a DIC (0.24 g; 1.89 mmol) and HOBt (0.25 g; 1.89 mmol) as the coupling reagents. After the last Fmoc deprotection as described above, the detachment of the peptides from the resin and the side-chain deprotection were performed simultaneously by treatment with a 50% TFA-5% anisole–5% TIS mixture in DCM for 2 h. The solutions were filtered from the resin and evaporated to dryness. The residues were triturated with tert-butyl-methylether, then dissolved in 1 M AcOH, and the solutions were lyophilized. The pentapeptides **1b–1g** and **2b, 2c** were purified by a preparative HPLC using the conditions described in the General methodologies section. The analytical HPLC retention times in minutes for the peaks of **1b** (8.45), **1c** (8.58), **1d** (8.62), **1e** (8.07), **1f** (8.13), **1 g** (8.58), **2b** (9.41) and **2c** (9.34) were recorded, using 15 × 0.4 cm, 5 μm Supelco column at a flow rate of 1 ml/min and a detection at 220 nm with a 5–100 % gradient of ACN in 0.05 aqueous TFA, for 40 min. For **1b–1g** ($C_{26}H_{35}N_5O_9$, 561.1), MS (m/z): 562.1 $(M + H)^+$ and for the **2b** and **2c** ($C_{26}H_{35}N_5O_9$, 559.1), MS (m/z): 560.1 $(M + H)^+$ were determined with the FAB technique (Micromass, Manchester, UK). A correct amino acid composition was found for all of the analogs prepared.

Preparation of the ^{3}H-labeled pentapeptides **3b**, **3c**

The tritiated pentapeptides **3b**, **3c** were obtained according to the procedure used for **3a** preparation (Hlaváček et al. 2007; Tykva et al. 2007), typically: the pentapeptide **2b** or **2c** was dissolved in N, N-dimethylacetamide, with a PdO/$BaSO_4$ catalyst (10% Pd) (Kuhn et al. 1955) being added, and this mixture was stirred in the original apparatus (Hanuš et al. 1971; Černý et al. 1981) with tritium gas containing 70% of $^{3}H_2$ at a pressure of 80 kPa, at room temperature for 2 h (Evans 1974). After solvent evaporation, the residue was suspended in water (0.5 ml) and the catalyst removed by centrifugation and washed using 0.5 ml of water. The combined supernatants were freeze-dried. The lyophilizate was purified by HPLC on a 25 × 0.4 cm column, 5 μm LiChrospher WP-300 RP-18 (Merck, Germany), with a flow rate of 0.6 ml/min, by an isocratic elution by a mixture of ACN in 0.05% aqueous TFA (ACN: 9%), the detection of products—by UV 210 nm and radioactivity. UV spectrophotometry (275 nm) was used for the determination of the mass of the products. Radioactivity was estimated by a liquid scintillation measurement. The purity was established by HPLC. Table 2 summarizes the conditions of labeling and characteristics of the labeled peptides.

Insect treatment

Females of *Neobellieria bullata*, Diptera (an approximate weight of 90 mg), raised at 25°C, with 12 h light/12 h dark cycles were used in the experiments. The larvae were

Table 2 Conditions of radiolabeling and characteristics of ^{3}H labeled peptides H-Tyr-D-Asp-[^{3}H]Pro-Ala-Pro-OH (**3b**) and H-Tyr-Asp-[^{3}H]Pro-D-Ala-Pro-OH (**3c**)

Peptide[a]	Precursor (mg)	Catalyst (mg)	Yield (mg) (Gbq)	Spec. activity (Tbq/mmol)	Radiochrom. purity (%)
3b	**2b;** 0.4	3.8	0.25 (0.69)	1.53	>97
3c	**2c;** 1.0	4.3	0.59 (1.72)	1.64	>97

[a] In N, N-dimethylacetamide solution with tritium gas containing 70% of $^{3}H_2$, at 80 kPa pressure at room temperature for 2 h, 10% PdO/$BaSO_4$ catalyst

raised on beef liver covered with sawdust (pupariation medium). The pupae were separated from the medium and placed into nylon cages before emergence. The flies were fed sugar and water for three days and from day 4 beef liver, which later served as an oviposition medium.

Peptides were injected in Ringer's solution (10 nmol in 5 μL/female) into the upper part of the thorax of the Et_2O-anesthesized 24–48 h-old flies. The treated female flies were placed into cages with untreated males and their ovaries were dissected 2, 4, 8 and 16 days later and examined for morphological and histological changes. The hatchability of the eggs in the uterus and the appearance of the eggs were evaluated in the first and second gonotrophic cycles. Each experimental group consisted of 50 flies.

Morphological assessment of the status of the ovaries

The dissected ovaries were spread on a microscopic slide in a physiological solution and microscopically examined for yolk deposition and oocyte growth. The different stages of yolk deposition were classified according to the scale (King 1970). The oocyte development was scored from 1 to 5, with 1 being no yolk in the oocyte, 2, 3 and 4 being oocyte with yolk filling up to a quarter, half and three-quarters of the egg chamber, respectively. Stage 5 indicates mature eggs ready to be deposited in the uterus. In the radioactivity incorporation assay, the small = 5th–6th and large = 11th–12th of the 14 developmental stages of yolk deposition in oocytes were estimated.

Hatchability assessment

The uterus content was examined before the time of the egg/larva deposition, and hatchability was expressed as the number of developed larvae in the uterus. The untreated flies deposited in the uterus 98–110 eggs, in which the segmented larvae were 95–98%. This corresponds to a hatchability of 95–98%.

Histological approach, assessment of the changes

Selected ovaries, in which visible changes in the morphology of the egg chambers were detected, were fixed in Bouin's solution, embedded in Paraplast (Sigma-Aldrich s.r.o., Czech Republic), and 5 μm sections were cut and stained with Mallory's or Mayer's hematoxyline. The sections were checked for changes in the follicular epithelium and the conditions of its nuclei, the yolk deposition, and its structure in the oocyte as well as the appearance of nutritive cells and their nuclei. These changes and their frequency were correlated with the intervals after each peptide application. The severity of the changes was assessed, as was the percentage of pathological changes in the egg chambers of the ovariole (Table 3).

In vitro application of radioactively labeled peptides

For the in vitro experiments, twelve dissected pairs of ovaries of identical stage and appearance from the 4-day-old females were placed into a solution of tritiated pentapeptide (1 μCi (37 kBq) in 5 μL of the physiological solution) in small embryo dishes at room temperature. Because of the different molar radioactivities of the corresponding compounds (Table 2), different amounts of each of the peptides were used: **3a** (16.88 ng), **3b** (13.57 ng) and **3c** (12.66 ng), based on the pentapeptides' molecular weight, 561.1. At time intervals of 5 min and 120 min, the ovaries were removed, washed twice in the physiological solution and two at one trial placed into individual scintillation vials and covered with 1 ml of NCS II tissue solubilizer, Amersham International. After one day, 10 ml of EcoLite liquid scintillator (ICN Biochemicals Inc.) were added and the radioactivity was determined in the Beckman 6500 spectrometer. The highest and lowest values of the sets were eliminated and the ten remaining samples were used for an evaluation of the mean values and their standard deviation. From three independent experiments, the total SD was calculated from ±15 to ±25%. Simultaneously, incubations for the selected time period were done for metabolite determination, and the samples were frozen until analyzed.

Extraction for the metabolite determination

An ice-cold solution (0.4 mL) of Complete Mini protease inhibitor cocktail (Roche Applied Sciences) was added (one tablet dissolved in 3.5 mL of 50 mM HEPES buffer,

Table 3 Larval hatching and resorption of oocytes after peptide administration

Peptide	Hatchability[a] (First gonotrophic cycle, %)	Resorption[b] (Second gonotrophic cycle, %)
H-Tyr-Asp-Pro-Ala-Pro-OH (5P), **1a**	20	20
H-D-Tyr-Asp-Pro-Ala-Pro-OH, **1b**	40	99
H-Tyr-D-Asp-Pro-Ala-Pro-OH, **1c**	50	80
H-Tyr-Asp-D-Pro-Ala-Pro-OH, **1d**	30	10
H-Tyr-Asp-Pro-D-Ala-Pro-OH, **1e**	30	30
H-Tyr-Asp-Pro-Ala-D-Pro-OH, **1f**	40	40
all-D-(H-Tyr-Asp-Pro-Ala-Pro-OH), **1g**	20	88

[a] Hatchability in the first gonotrophic cycle is given only as in the second gonotrophic cycle no hatchability was observed

[b] The difference to 100% is equal to yolk content in egg. 100% resorption means no egg yolk. Resorption influences the embryogenesis, which results in zero hatchability

pH 7.6) to the frozen, pooled ovaries in an Eppendorf tube and the content was homogenized for 1 min using a teflon pestel. After centrifugation, the supernatant was removed and either immediately analyzed by radio-HPLC or frozen and analyzed later.

Analysis of the metabolites of pentapeptides **3a–3c** (Figs. 2, 3, 4)

All of the radio-HPLC analyses were performed using the Waters liquid chromatograph (Waters, USA). A programmable UV detector was connected online to a radiometric flow-through detection system (Beckman 171, http://www.beckman.com). The LiChroCART stainless steel analytical column (250 × 4 mm; Merck, http://www.merck.com.), packed with a LiChrosphere WP-300, with a particle size of 5 µm was used. The column was protected with a guard column (4 × 4 mm), packed with a LiChrosphere 100 RP-18, using a particle size of 5 µm (Merck). The mobile

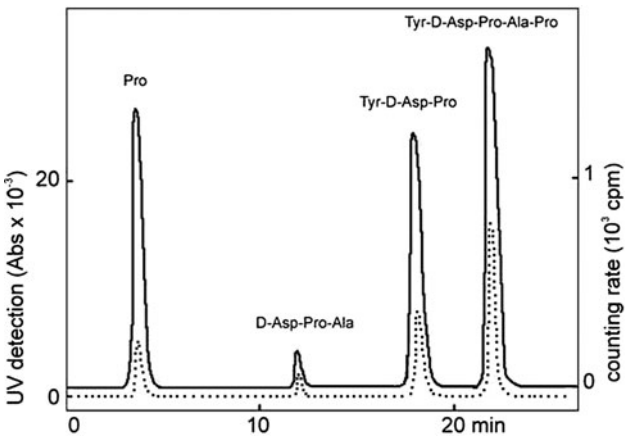

Fig. 2 The radio-HPLC (*full line*) of the pentapeptide **3b** after a 25-min incubation with the ovaries of the flesh fly *Neobellieria bullata* and the UV-HPLC (*dotted line*) of the corresponding non-labeled fragment standards

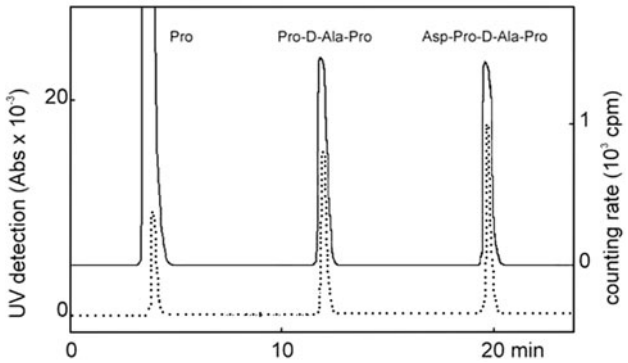

Fig. 3 The radio-HPLC (*full line*) of the pentapeptide **3c** after a 25-min incubation with the ovaries of the flesh fly *Neobellieria bullata* and the UV-HPLC (*dotted line*) of the corresponding non-labeled fragment standards

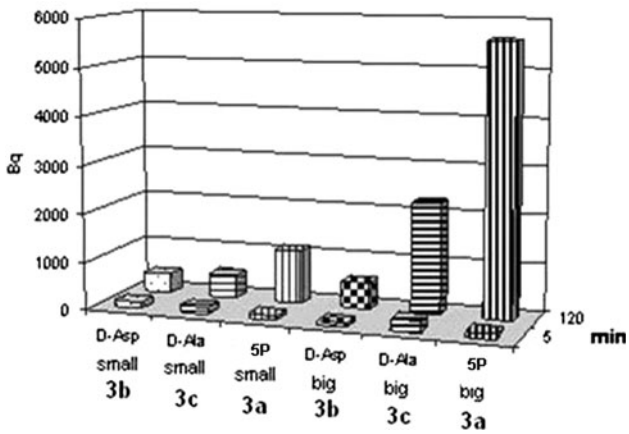

Fig. 4 The incorporation of radioactivity into the ovaries of the flesh fly *Neobellieria bullata* after incubation with the H-Tyr-Asp-[^{3}H]Pro-Ala-Pro-OH (**3a**), H-Tyr-**D-Asp**-[^{3}H]Pro-Ala-Pro-OH (**3b**) and H-Tyr-Asp-[^{3}H]Pro-**D-Ala**-Pro-OH (**3c**) pentapeptides. The "small" and "large" mean the 5th–6th and 11th–12th, respectively, of the 14 developmental stages of the oocytes based on the deposition of the yolk (King 1970)

phase was composed of the aqueous phase (0.035% TFA in redistilled water) and the organic phase (0.05% in ACN). After passing through the UV detector, the eluent was continuously mixed with the Ready Safe liquid scintillator (Beckman Coulter, USA) in a ratio of 1:2.5 (v/v) in an online mixer. The mixture ran through a 500-μL detection cell. The radiometric detector threshold was set at 0.02%. The UV detector was set at 230 nm with 0.05 AUFS. The separation was performed at ambient temperature using a 30-min linear gradient from 0 to 30% of the organic phase using a flow rate of 0.8 mL/min and continuous degassing with helium. A sample volume of 20–80 μL was used. The area of each peak was evaluated as the ratio of its counting rate (cpm) to the totally measured sum of the counting rate in all of the peaks of the appropriate radiochromatogram (relative concentration c_{rel} in percentage). The stability of the radiolabeled pentapeptides was checked before each experiment.

The samples were centrifuged for 5 min and an aliquot of the supernatant was analyzed. The standard unlabeled peptides (Hlaváček et al. 2007) and proline were detected by UV spectrometry; their retention times were compared to those of the peaks in the radiochromatogram. The retention times of the radioactive fractions were corrected to the time delay between the UV and the radiometric detector (0.55 min). The precision of the method was expressed as the coefficient of the variation in percentage, which fluctuated from 1.3 to 7.7%. It was determined by analyzing five replicates of the same biological sample within 1 day.

The extraction procedure recovery was evaluated using pentapeptide **3a** calibration solutions of three different concentrations (42, 150 and 370 kBq/mL) by a comparison of the extracted and applied radioactivity. The average recovery was between 86.6 and 97.2% ($n = 4$) with a precision range from 3.3 to 5.2 (% coefficient of variation). The linearity of the radiometric detector response was verified using **3a** calibration solutions in the range of 0.2–10 kBq with an average correlation coefficient of 0.997 ($n = 4$). The absolute detection limit in the system, defined by a signal-to-noise ratio of 3, was assigned for **3a** in the range of 85–150 Bq, which corresponds to 59–104 (rounded to 60–100) fmol.

The NMR structure determination

The spectra were measured on a Bruker AVANCE-II instrument using a cryo-probe (^{1}H at 600.13 MHz; ^{13}C at 150.9 MHz frequency) in DMSO-d6. The series of proton 1D, 2D-COSY, 2D-TOCSY (spin-lock time 90 ms) and 2D-ROESY (mixing time 300 ms) was measured at 27°C for the complete structural assignment of the proton signals. The structural assignment of the carbon-13 signals was achieved by combining the 1D-APT, 2D-H, C-HSQC and 2D-H,C-HMBC spectra. The temperature coefficients of the amide NH protons were obtained from the 1D-proton spectra measured at 27, 37 and 47°C.

Results and discussion

The assay of the oostatic activity of the pentapeptides **1b**–**1g** with D-amino acids in the peptide chain has shown a significant decrease of hatchability in the first gonotrophic cycle, which was comparable with that of the parent pentapeptide **1a**, and no hatchability in the second gonotrophic cycle (Table 3).

The morphological changes in ovaries correspond to a large resorption of the oocytes of treated flies after the application of the pentapeptides **1b**, **1c** and **1g**. Even if the pentapeptides **1d**–**1f** exhibit low resorption, this effect still interferes with the embryogenesis, so that hatching is impossible. Thus, the changes in the female reproductive system of *N. bullata*, after the application of the pentapeptides assayed, are degenerative and correspond to the histological pictures shown in Fig. 1. The strong oostatic activity of the all D-amino acids containing peptide **1g** speaks in favor of the suggestion that the effect of oostatic peptides in *N. bullata* is complex and proceeds without involvement of a specific receptor (Bennettova et al. 2010). Rather an intake of the analyzed sequences into the intercellular spaces between follicular cells could be assumed. This intake increases with continuous yolk deposition even if the mechanism responsible for the oostatic peptide transport has yet to have been found (Slaninová et al. 2007).

Moreover, a majority of the effects occurred not in the first but in the second gonotropic cycle (approximately sixteen days after eclosion). The second gonotrophic cycle (the one more affected) starts several days after the peptide application, and it seems improbable that the peptide would persist in active concentration so long considering that its half-life is in the order of tens of minutes.

With the aim of explaining the action of the oostatic peptides in *N. bullata*, we have also performed studies on the degradation and accumulation of tritiated pentapeptides in the ovaries of this insect. For these studies, we have chosen the parent pentapeptide **1a** (radioactive form **3a** assayed) and its analogs **1c** and **1e** (radioactive forms **3b** and **3c**) containing D-amino acid residues located in the neighborhood of the tritiated central Pro residue [^{3}H]Pro^{3}. In these analogs, the D-Asp^{2} residue is linked by its N-terminus to a Tyr residue in position 1 and the D-Ala^{4} residue by its C-terminus to Pro residue in position 5. In such an arrangement, the degradation of the pentapeptides **3a**–**3c** and the radioactivity accumulation could be evaluated via the whole pentapeptide sequence.

A slower degradation of the parent peptide **1a** in the ovaries in comparison with the hemolymph (Tykva et al.

2007) suggests the participation of different enzymatic systems for the degradation of this peptide in the two organs. Therefore, our initial study with the D-amino acid containing analogs followed a degradation and accumulation of the corresponding pentapeptides in the ovaries.

Contrary to the quick degradation of the peptide **1a** (radioactive form **3a** assayed) in the ovaries of *N. bullata* (Bennettová et al. 2010), its analogs **1c** and **1e** (radioactive forms **3b** and **3c**), owing to the presence of the D-Asp^2 and D-Ala^4 residues, respectively, were degraded much more slowly. Apparently, the proteolytic enzymes must handle an opposite orientation of the side-chains, which change the conformation of the corresponding pentapeptide (see the discussion of the NMR spectra below). Figure 2 shows that 120 min after the incubation with the ovaries, the pentapeptide **1c** (radioactive pentapeptide **3b**) and its degradation product Tyr-D-Asp-Pro are still present in the ovaries as detected by radio-HPLC (full line). Similarly, as shown in Fig. 3, the pentapeptide **1e** (radioactive pentapeptide **3c**) degrades slowly within the same period of time to Asp-Pro-D-Ala-Pro and Pro-D-Ala-Pro (full line). Using UV-HPLC, the corresponding peaks of the non-labeled standards (Tykva et al. 2007) of the degradation products were detected (dotted lines). However, the degradation of the pentapeptide **1e** (radioactive **3c**) to the final [^{3}H]Pro in position 3 is significantly quicker than that of the pentapeptide **1c** (radioactive **3b**).

As far as the total accumulation of radioactivity is concerned, the incubation of *N. bullata* ovaries with the labeled pentapeptides **3a–3c** showed similarly different results. The significantly decreased uptake of radioactivity from peptides **3b** and **3c** into the ovaries in comparison with that of the parent peptide **3a** (Fig. 4) could be connected with an increased stability of the relevant peptide bonds in pentapeptides with D-Asp^2 and D-Ala^4 toward the corresponding proteolytic enzymes.

The relatively large difference in the radioactivity incorporation between the two analogs **3b** and **3c** could be explained by the different effect of the D-Asp^2 and D-Ala^4 residues on the conformation of the N-terminal part of the pentapeptides. Tyr in position 1 is believed to start a very quick metabolic cleavage of the parent 5P (**1a**) in the ovaries, with the final release of [^{3}H]Pro^3 (Bennettová et al. 2010). Owing to the impaired ability of proteolytic enzymes to recognize the area around the peptide bond Tyr-D-Asp^2, this cleavage and consequently the penetration of the released [^{3}H]Pro^3 into the ovaries is more strongly decreased with pentapeptide **3b** as compared to **3c**.

With the aim of rationalizing the results of the degradation and incorporation studies with the pentapeptides **1a**, **1c** and **1e**, we studied these peptides using NMR spectroscopy. The presence of two proline residues in the peptides **1a**, **1c**, **1e** leads to the appearance of four isomeric species in solution because of the population of *trans*- and *cis*-isomers on both the Asp-Pro and Ala-Pro peptide bonds. The isomers can be distinguished by the NOE contacts observed in the 2D-ROESY spectra: the NOE contact between the H$^\alpha$ of Asp or Ala and the H$^\delta$ of Pro indicates a *trans*- X-Pro bond and the NOE contact between the H$^\alpha$ of Asp or Ala and the H$^\alpha$ of Pro indicates a *cis*- X-Pro bond (Fig. 5).

The equilibrium population of the individual isomers (*trans-/trans-, cis-/trans-, trans-/cis- and cis-/cis-*) observed in the peptides **1a**, **1c** and **1e** is shown in Table 4. It can be seen that an isomer with both *trans*-peptide bonds is preferred in all of the studied peptides while the isomer with both *cis*-peptide bonds has the lowest population. The presence of D-Asp or D-Ala leads to a significant increase of the isomer with *cis*-D-Asp-Pro in **1c** (29 %) and *cis*-D-Ala-Pro in **1e** (27 %), which, along with a lower population of the *trans-/trans* isomer (62 % in **1c** and 52 % in **1e**), can be responsible for the slower enzymatic degradation of **1c** and **1e**. The fastest step of degradation (the splitting of the Tyr-Asp peptide bond—see above) can explain the difference between the rates of degradation of **1c** and **1e**.

Since the presence of four isomers significantly complicates the analysis of the NMR spectra, a complete structural assignment of all of the signals (^{1}H and ^{13}C) was performed only for the major *trans-/trans-* isomers. Their NMR data are summarized in Table 5.

For an estimation of the effect of the presence of the D-residue in position 2 (in **1c**) and in position 4 (in **1e**) on the molecular geometry, we have constructed models of **1a**, **1c** and **1e** using extended β-sheet parameters for all of the residues. The presence of two Pro residues partially distorts the regular β-sheet chain. We have therefore applied unrestrained geometry optimization to minimize the energy of the model structures using the AMBER version of the Hyperchem package. The calculated structures for **1a**, **1c** and **1e** using the carbon atoms of the Asp-Pro peptide bond (C=O of Asp-2 and C$^\alpha$, C$^\delta$ of Pro-3 for the structure overlap) are shown in Fig. 6.

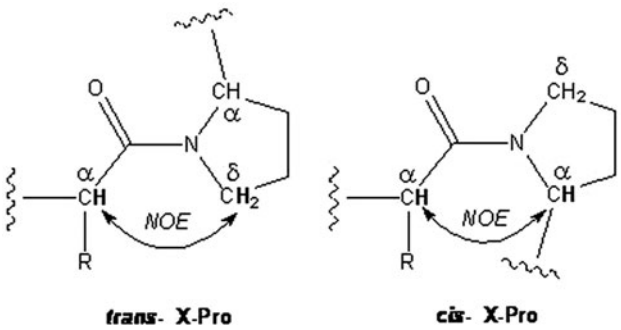

Fig. 5 A schematic diagram for distinguishing the *trans*- and *cis*-X-Pro peptide bonds from the characteristic NOE contacts

Table 4 Equilibrium population of isomers with *trans*- and *cis*-X-Pro bonds in peptides **1a**, **1c** and **1e** observed in DMSO-d6 at 27°C

Configuration on peptide bond		**1a**	**1c**	**1e**
Asp-Pro	Ala-Pro	(all-L)	(D-Asp)	(D-Ala)
trans-	*trans*-	71%	62%	52%
cis-	*trans*-	11%	29%	12%
trans-	*cis*-	10%	6%	27%
cis-	*cis*-	8%	3%	9%

The linear pentapeptides **1a**, **1c** and **1e** are expected to exist in solution as flexible molecules. Table 5 shows a close similarity of the majority of the proton NMR parameters in **1a**, **1c** and **1e**. The observed coupling constants $J(N,\alpha) = 7.8–8.6$ Hz are in the range of the random-coil values, the temperature coefficients $\Delta\delta NH/\Delta T$ of the Asp[2] (−3.8 to −4.2 ppb) indicate a moderate solvent shielding of the NH, and those of the Ala[4] (−5.0 to −7.4 ppb) suggest the NH exposed to a bulk solvent. There is no evidence for a strong solvent shielding or an H-bonding of the peptide NH protons. The observed NOE contacts are the most important parameters used in the conformation analysis of the peptides in solution. Their application for non-rigid molecules is not straightforward, since the observed NOEs can come from different conformations present in solution. The situation in our case is further complicated by a partial overlap of some signals of the major and minor isomers that make the correct assignments of the weak NOE crosspeaks in the 2D-ROESY

Table 5 Proton and carbon-13 NMR data of peptides H-Tyr-Asp-Pro-Ala-Pro-OH (**1a**), H-Tyr-D-Asp-Pro-Ala-Pro-OH (**1c**) and H-Tyr-Asp-Pro-D-Ala-Pro-OH (**1e**) in DMSO at 27°C

Residue	Parameter	**1a**	**1c**	**1e**	Parameter	**1a**	**1c**	**1e**
Tyr-1	NH	8.09	8.11	8.013	CO	167.93	167.95	167.82
	J(N,α)	*a*	*a*	*a*	Cα	53.56	53.78	53.51
	Hα	3.905	3.92	3.915	Cβ	36.18	36.62	36.14
	J(α,β)	5.8; 7.4	5.8; 8.1	6.2; ~7.0	C1	124.71	124.88	124.65
	Hβ1, Hβ2	2.94; 2.82	2.92; 2.81	2.93; 2.82	C2,C6	130.70	130.82	130.68
	J(β1,β2)	14.2	14.2	14.2	C3,C5	115.45	115.52	115.40
	H-2,6	6.985	7.04	6.97	C4	156.80	156.82	156.80
	H-3,5	6.68	6.70	6.67				
	OH	9.40	9.43	9.42				
Asp-2	NH ($\Delta\delta NH/\Delta T$)	8.91 (−4.2)	8.87 (−3.8)	8.91 (−3.8)	CO	168.62	168.17	168.78
	J(N,α)	7.8	8.6	8.0	Cα	47.70	47.17	47.43
	Hα	4.82	4.89	4.83	Cβ	36.10	36.62	36.14
	J(α,β)	6.4; 7.2	8.4; 6.1	6.8; *a*	COOH	171.64	171.76	171.99
	Hβ1, Hβ2	2.76; 2.46	2.63; 2.22	2.82; 2.50				
	J(β1,β2)	16.9	16.4	16.7				
	COOH	12.47	~12.40	12.46				
Pro-3	Hα	4.30	4.29	4.28	CO	170.80	171.12	170.40
	$H_2\beta$	1.96; 1.84	2.01; 1.78	1.90; 1.79	Cα	59.49	59.43	60.06
	$H_2\gamma$	1.84; 1.80	~1.82 (2H)	~1.79 (2H)	Cβ	29.25	29.46	29.73
	$H_2\delta$	3.56; 3.38	3.65; 3.58	3.64; 3.42	Cγ	24.75	24.75	24.10
					Cδ	46.88	47.08	46.53
Ala-4	NH ($\Delta\delta NH/\Delta T$)	7.97 (−5.6)	8.06 (−7.4)	7.535 (−5.0)	CO	170.41	170.80	170.15
	J(N,α)	7.5	7.3	8.4	Cα	46.22	46.20	46.02
	Hα	4.46	4.44	4.60	Cβ	16.92	17.00	17.59
	J(α,β)	7.0	7.0	6.9				
	$H_3\beta$	1.165	1.19	1.13				
Pro-5	Hα	4.21	4.23	4.18	COOH	173.49	173.39	173.46
	$H_2\beta$	2.13; 1.83	2.13; 1.87	2.13; 1.825	Cα	58.70	58.70	58.95
	$H_2\gamma$	1.90; 1.83	~1.87 (2H)	~1.89 (2H)	Cβ	28.78	28.77	28.86
	$H_2\delta$	3.59; 3.475	3.58; 3.52	3.61; 3.50	Cγ	24.35	24.42	24.61
	COOH	12.47	~12.40	12.46	Cδ	46.40	46.57	46.94

[a] The J-value was not determined

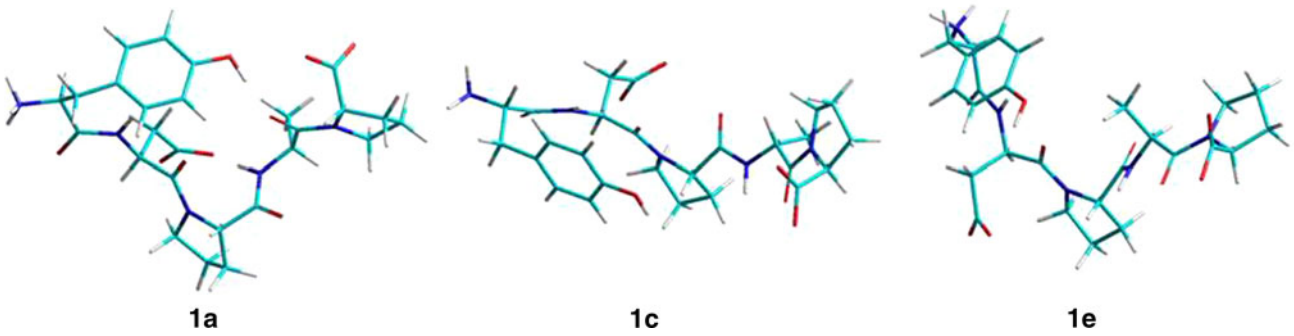

Fig. 6 The unrestrained geometry optimized structures of the H-Tyr-Asp-Pro-Ala-Pro-OH (**1a**), H-Tyr-**D-Asp**-Pro-Ala-Pro-OH (**1c**) and H-Tyr-Asp-Pro-**D-Ala**-Pro-OH (**1e**) pentapeptides

Fig. 7 A schematic diagram of the observed inter-residue NOEs in the H-Tyr-Asp-Pro-Ala-Pro-OH (**1a**), H-Tyr-**D-Asp**-Pro-Ala-Pro-OH (**1c**) and H-Tyr-Asp-Pro-**D-Ala**-Pro-OH (**1e**) pentapeptides

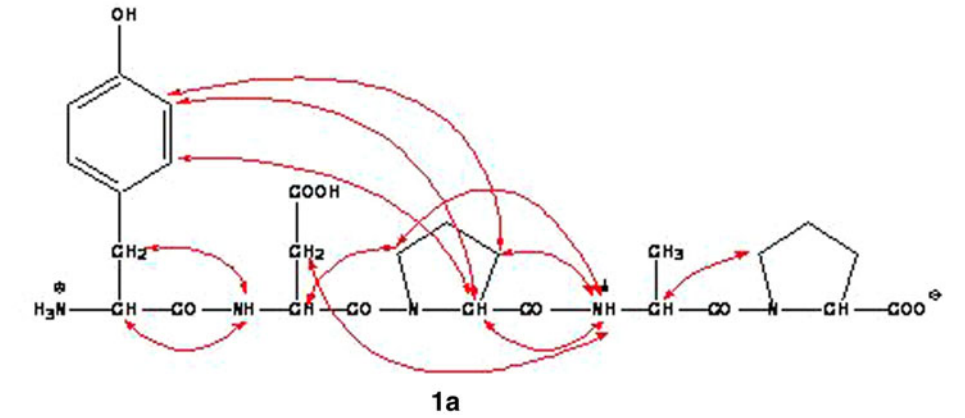

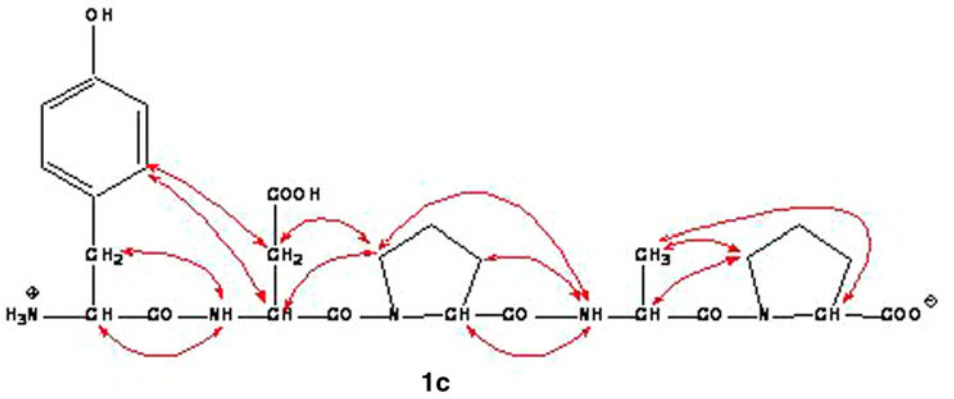

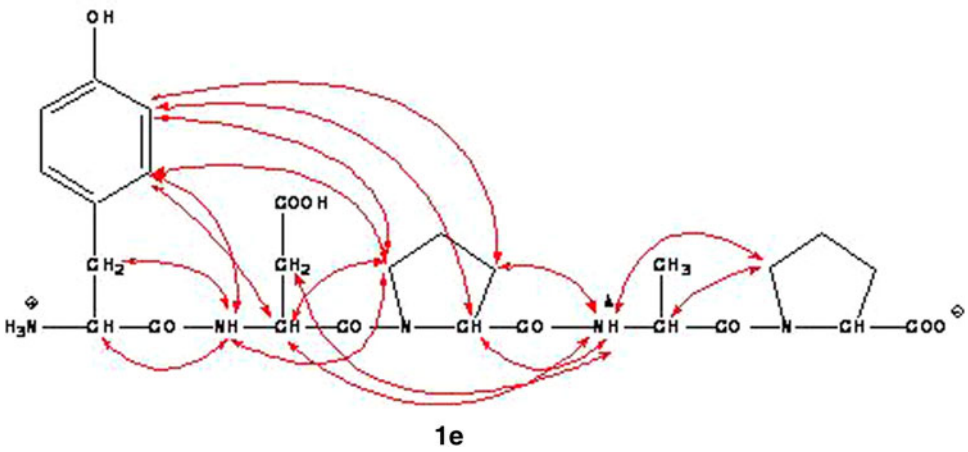

spectra difficult. Therefore, we have selected only unambiguously assignable inter-residue strong and medium cross-peaks from the ROESY spectra, which are shown schematically in Fig. 7. While the NOEs between the protons of neighboring residues (sequential NOEs) can usually be observed in all of the even non-structured flexible peptides, the observations of medium-range (non-sequential NOEs) are taken as indicators of the presence of the population of some secondary structure fragments. As can be seen in Fig. 7, there are only sequential NOEs identified in **1c** but some additional non-sequential NOEs (between the protons of Tyr^1/Pro^3 and Asp^2/Ala^4) in **1a** and **1e**. We have tried to use all of the NOEs shown in Fig.7 as distance restraints and apply them on previously unrestrained optimized structures (Fig. 6). An energy minimization (AMBER; for all of the NOE restraints, the upper distance limit was 4 Å) provided structures with markedly higher energy and some torsion angles out of the allowed regions. It seems obvious that these peptides adopt not only one preferred conformation in solution but some conformation families contributing to the overall observed NOEs. The analysis combining molecular dynamics to identify the conformation families, a detailed analysis of the integrated NOE values, and back calculations of the relaxation matrices will be the subject of a future paper.

Conclusion

The introduction of D-amino acids into the oostatic peptide **1a** retained the oostatic activity and enhanced the resorption of the developing eggs in *N.bullata*. As no receptors have yet been found (Slaninová et al. 2004), an autonomous function of the ovaries in the process of active intake by passing peptides through the inter-spaces of the follicular cells could be proposed. D-amino acid-containing analogs efficiently interfere with an enzymatic system, which very effectively degrades the parent pentapeptide **1a** during its transport into the egg chamber. Contrary to the parent pentapeptide **1a**, the D-Asp^2- or D-Ala^4-containing isomers **1c** and **1e**, assayed for their degradation and radioactivity incorporation into ovaries as the radiolabeled forms **3b** and **3c**, were degraded much more slowly owing to a decrease of the respective peptide bonds cleavage. The increased stability (with the D-Asp^2 pentapeptide **1c** priority) thus also results in a retardation of the incorporation of the radioactivity of [^{3}H]Pro into the ovaries. The NMR spectra showed that the presence of D-Asp or D-Ala leads to a significant increase of the isomer with *cis*-D-Asp-Pro in **1c** (29%) and *cis*-D-Ala-Pro in **1e** (27%), which, along with the lower population of *trans-/trans* isomer (62% in **1c** and 52% in **1e**), can be responsible for the slower enzymatic degradation of **1c** and **1e**.

In general, the enhanced stability of the oostatic analogs after the introduction of D-amino acid residues is reflected in the prolonged half-life of the corresponding pentapeptides. Thus, more oocytes might be affected during the period of their development, which enhances the regulatory potency of the majority of the analogs.

Acknowledgments This research was supported by Research Project Z4 055 0506 and the Czech Science Foundation No. 203/06/1272.

References

Barlos K, Chatzi O, Gatos D, Stavropoulos G (1991) 2-Chlorotrityl chloride resin. Int J Peptide Protein Res 37:513–520

Bennettová B, Hlaváček J, Tykva R (2002) Follicular epithelium changes after application of insect oostatic hormone analogues in *Neobellieria bullata* (Diptera). In: Abstract book of VIIth European Congress of Entomology, October 7–13, 2002 Thessaloniki, Greece. Abstract No 10: p. 25. Hellenic Entomological Society 2002

Bennettová B, Slaninová J, Vlasáková V, Hlaváček J, Holík J, Tykva R (2010) J Insect Sci 10:48. http://insectscience.org/10:48

Borovsky D, Carlson DA, Griffin PR, Shabanovicz J, Hunt DF (1990) Mosquito oostatic factor: a novel decapeptide modulating trypsin-like enzyme biosynthesis in the midgut. FASEB J 4:3015–3020

Černý B, Hanuš J (1981) Tritium incorporation into solvents under the conditions of catalytic dehalogenation. J Label Comp 18:947–954

Hanuš J, Vereš K (1971) Preparation of tritium labeled D, L-2, 6-diaminopimelic acid. J Label Comp 7:425–430

Hlaváček J, Bennettová B, Barth T, Tykva R (1997) Synthesis, radiolabelling and biological activity of peptide oostatic hormone and its analogs. J Peptide Res 50:153–158

Hlaváček J, Tykva R, Bennettová B, Barth T (1998) The C-terminus shortened analogs of the insect peptide oostatic hormone with accelerated activity. Bioorg Chem 26:131–140

Hlaváček J, Mařík J, Konvalinka J, Bennettová B, Tykva R (2004) Synthesis and application of methyleneoxy pseudodipeptide building blocks in biologically active peptides. Amino Acids 27:19–27

Hlaváček J, Černý B, Bennettová B, Holík J, Tykva R (2007) Preparation of tritiated oostatic peptides for study of radioactivity incorporation in flesh fly *Neobellieria bullata*. Amino Acids 33:489–497

King RC (1970) Ovarian development in *Drosophila melanogaster*, pp 33–54. Academic Press, New York

Kuhn R, Haas HJ (1955) Braunes Palladiumoxydhydrat-bariumsulfat fűr katalytische Hydrierungen. Angew Chem 67:785

Mařík J, Bennettová B, Tykva R, Buděšínský M, Hlaváček J (2001) Synthesis and effect of shortened oostatic decapeptide (TMOF) analogs with isosteric structures on reproduction of *Neobellieria bullata*. J Peptide Res 57:401–408

Slaninová J, Bennetová B, Nazarov ES, Šimek P, Holík J, Vlasáková V, Hlaváček J, Černý B, Tykva R (2004) Activity and mechanism of action of insect oostatic peptides in flesh fly. Bioorg Chem 32:263–273

Tykva R, Hlaváček J, Němec V, Bennettová B (1999) Effect of a peptide and some of its analogs on the reproduction of *Sarcophaga bullata* and *Locusta migratoria*. In: Del Re AAM, Brown C, Capri E, Errera G, Evans SP, Trevisan M (eds) Human and environmental exposure to xenobiotics. La Goliardica Pavese, Pavia, pp 895–901

Tykva R, Hlaváček J, Bennettová B, Slaninová J, Novák J, Němec V, Černý B, Vlasáková V, Holík J (2007a) Conditions of elimination of environmental pollution in insect management. In: Book of abstracts of the 14th international symposium on environmental pollution and its impact on life in the Mediterranean region with focus on environment and health, October 10–14, 2007. Sevilla, Spain, p 407

Tykva R, Hlaváček J, Vlasáková V, Černý B, Borovičková L, Bennettová B, Holík J, Slaninová J (2007b) Radiochromatographic assay of metabolites of the oostatic peptide labeled in different positions of the peptide chain. J Chrom B 848:258–263